Temperature and Salt Addition Effect on the Micellized Radical Pairs Recombination Studied by Stimulated Nuclear Polarization

N. V. Lebedeva, E. G. Bagryanskaya,* V. R. Gorelik, I. V. Koptyug, and R. Z. Sagdeev

International Tomography Center, SB RAS, Novosibirsk, Russia

Received: December 13, 2000; In Final Form: February 20, 2001

It was found that the shape of the ^{13}C stimulated nuclear polarization (SNP) spectra, detected in the photolysis of dibenzyl ketone (DBK) and α-methyldeoxybenzoine (MDB), exhibits a noticeable temperature dependence. For the relatively large sodium dodecylsulfate (SDS) micelles, the temperature increase leads to the increase in the line width of SNP spectra, while in the smaller sodium octylsulfate (SOS) micelles the splitting in the SNP spectra decreases. From the comparison of the experimental data with the model calculations based on the numerical solution of the Liouville equation, the influence of the temperature and salt additions on the collision rate of radicals in micelle interior was evaluated. The obtained activation energy of the translational diffusion of small radicals is $E_a = 6.7 \pm 0.25$ kcal/mol and $E_a = 5.6 \pm 0.2$ kcal/mol for SDS and SOS micelles, respectively. Additionally, the influence of temperature and salt additions on the lifetime of the micellized radical pairs (RPs) formed in the photolysis of MDB and DBK has been studied experimentally. It is shown that the temperature dependence of the RP lifetime is determined mainly by the changes in the escape rate.

Introduction

Micelles represent a simplified model of biological membranes; therefore, significant effort is devoted to establishing their properties and structure. The micelles can serve as "limited volume microreactors" for radical reactions. A large number of studies published during the past few years report the observation and investigation of the magnetic and magnetic isotope effects, very strong nuclear and electron spin polarization and other phenomena for the radical pairs confined within micelles.[1−15] Investigation of the micellized radical pairs (RPs) attracts significant attention since the intersystem crossing in such RPs is critically affected by the exchange interaction and electron spin relaxation. This opens up the possibility to study both the exchange interaction and its influence on the intersystem crossing of RPs. The spin dynamics and chemical kinetics of micellized RPs have been studied by a number of techniques, e.g., MARY,[3] TR EPR,[5,8] CIDNP,[9] RYDMR,[3,10] PYESR,[11,12] SNP,[13−16] etc.

It has been shown earlier[13−16] that the application of the SNP technique to the study of spin dynamics and chemical kinetics of the RPs confined within the micelles allowed obtaining the parameters of exchange interaction for a number of RPs for measuring their lifetimes and making conclusions about the mechanism of electron spin relaxation. In the SNP technique, the resonant microwave field affects the rate of singlet−triplet conversion within RPs and thereby alters the measured polarization of nuclear spins in diamagnetic reaction products. The SNP spectra essentially represent the EPR spectra of RPs; therefore, they are more sensitive to the effects of the exchange interaction and spin-selective decay on the intersystem crossing within the micellized RPs than the CIDEP technique, which mostly reflects the contribution of free radicals. It has been demonstrated earlier[13,14] that the SNP spectra of micellized RPs under some conditions are sensitive to the reencounter frequency of the radicals, which depends on the micelle size and intramicellar viscosity. The size, shape, and aggregation number of micelles depend on the structure of the detergent molecules and its concentration, the concentration of a salt, the temperature, etc.[17−20] All previous SNP studies of micellized RPs have been performed at room temperature. Since the temperature change alters the micelle size and intramicellar viscosity and therefore affects the reencounter frequency, the shape of the SNP spectra is expected to exhibit a pronounced temperature dependence in the cases when the time of radical reencounters is comparable with time of triplet−singlet conversion.

The influence of temperature and salt additions on micelle size has been investigated in detail using various techniques (quenching of a luminescent probe,[21] spin-probe method,[19,22] small-angle neutron scattering,[23] and quasielastic light-scattering[17,20]). The results obtained by different techniques are in a good agreement with each other. This is not the case for the measurements of intramicellar viscosity. A considerable polydispersity of the micelles leads to very different values of their microviscosity, depending on the measurement.[24−31]

The aim of this work was to investigate the effect of the temperature and salt additions (NaCl) on the recombination of micellized RPs. This was achieved through the analysis of the SNP spectra of model RPs formed upon photolysis of α-methyldeoxybenzoin (α-MDB) and dibenzyl ketone (DBK) in alkyl sulfate micelles of different sizes (sodium dodecylsulfate (SDS) and sodium octylsulfate (SOS)). The comparison of experimental and calculated SNP spectra and kinetics allows us to study the changes in the rate of reencounters of radicals in micelles with temperature and salt additions. Using literature data on aggregation number at different temperature and salt concentration, we have obtained the temperature and salt additions dependence on the translational diffusivity of radicals inside the micelle.

* To whom correspondence should be addressed. Fax:007-3832-331399. Email: Elena@tomo.nsc.ru.

10.1021/jp004481k CCC: $20.00
Published on Web 04/21/2001

Experimental

The experimental SNP setup has been described earlier.[16] The reaction mixture was irradiated by laser pulses (Lambda Physik COMPex, $\lambda = 308$ nm, 20 Hz, 40 mJ) in RF cavity ($f = 1530$ MHz), located in the field of a magnet (0−78 mT). A flow system was used to transfer the irradiated mixture to the probe of a Bruker MSL-300 NMR spectrometer. In time-resolved experiments, the dependence of the polarization on variable time delay between a laser pulse and a RF pulse has been investigated. The duration of the RF pulse was 5 μs and the RF pulse edge was 20 ns. For the experiments to be performed at temperatures above or below the room temperature, the sample resided within a stream of warm air or cold nitrogen gas, respectively. The temperature within the sample cell was monitored by means of a calibrated thermocouple.

The detergent concentrations used in the experiments were [SDS] = 0.1 M and [SOS] = 0.2 M. The α-methyldeoxybenzoin (MDB) and dibenzyl ketone (DBK) concentrations were 3.1 mM for SDS and 7.4 mM for SOS solutions. The solubility of MDB and DBK as well as similar ketones in water solution is negligible. The fact that nearly 99% of MDB and DBK molecules react inside micelle interior is confirmed by the tremendous increase in the yield of cage products of triplet RPs in the photolysis of micelle solution in comparison with homogeneous solution.[32]

Results

DBK and MDB undergo homolytic α-cleavage upon photoexcitation to generate the RPs comprising phenacyl/benzyl and benzoyl/sec-phenethyl radicals, respectively.[33,34] Inside the micelle, the RP formed in DBK photolysis can recombine with the formation of the initial ketone or *p*-tolylbenzyl ketone. Phenacyl radical undergoes carbon monoxide elimination, with a rate which depends on the solvent polarity and temperature[35] and is equal to 6.4×10^6 s^{-1} at room temperature in benzene.[36] Recombination of the second RP leads to formation of dibenzyl. The RP formed during the photolysis of MDB may (1) recombine to regenerate the substrate, (2) disproportionate to produce styrene and benzaldehyde, (3) recombine in a head-to-tail fashion followed by an H shift to give *p*-ethylbenzophenone, or (4) escape from the micelle into the bulk aqueous phase. Reactions 1−3 have been shown to occur only within the micelle interior.[37,38] The lifetime of the triplet MDB molecule has been estimated as $\tau_T = 40 \pm 10$ns.[39]

In both reactions, the CIDNP and SNP spectra and kinetics have been detected by the ^{13}C NMR signal of the carbonyl carbon ($\delta = 198.4$ ppm) of initial ketone. After salt (NaCl) addition, the SNP spectra have been detected also by ^{13}C (II) of phenyl group of DBK as well as CO during the photolysis of DBK in SDS solution (Figure 1). The hyperfine interaction (hfi) constants of carbonyl ^{13}C in phenacyl and benzoyl radicals are 12.4 mT and 12.38 mT,[40] respectively, and are much larger than all other hfi constants (benzyl radical: $2A(CH_2) = 1.628$ mT, $2A(H_{ortho}) = 0.515$ mT, $2A(H_{meta}) = 0.179$ mT, $A(H_{para}) = 0.617$ mT; α-methylbenzyl radical: $3A(CH_3) = 1.63$ mT, $2A(H(\alpha)) = 1.79$ mT, $2A(H_{ortho}) = 0.49$ mT, $2A(H_{meta}) = 0.17$ mT, $A(H_{para}) = 0.61$ mT).[40] There is no experimentally measured data for the ^{13}C (II) hfi constant of benzyl radical; thus, we used the computed value (−1.4 mT) given in the paper of Turro et al.[41]

Temperature Dependence of CIDNP and SNP Spectra. Panels a and b of Figure 2 show the magnetic field dependencies of CIDNP detected upon photolysis of MDB in SDS and SOS micelles, respectively. It can be seen that as the temperature decreases, the maxima of the absolute polarization magnitude shift toward lower fields for both SOS and SDS micelles. The CIDNP in micellized RPs is known to arise due to the T$_{-}$α-Sβ transitions, which proceed in the S-T$_{-}$ level crossing region; therefore, the exchange interaction plays the key role in the CIDNP formation. It has been demonstrated earlier,[9,13,14] that for smaller micelles the maximum of the absolute polarization magnitude in the CIDNP magnetic field dependencies is observed in higher fields, which has been interpreted as an evidence of a stronger average exchange interaction in smaller micelles. Thus, the qualitative analysis of the temperature effect on the CIDNP dependencies leads to the conclusion that the effective exchange interaction increases at higher temperatures.

The ^{13}C SNP spectra detected by the NMR line of the carbonyl carbon upon photolysis of MDB in SDS and SOS

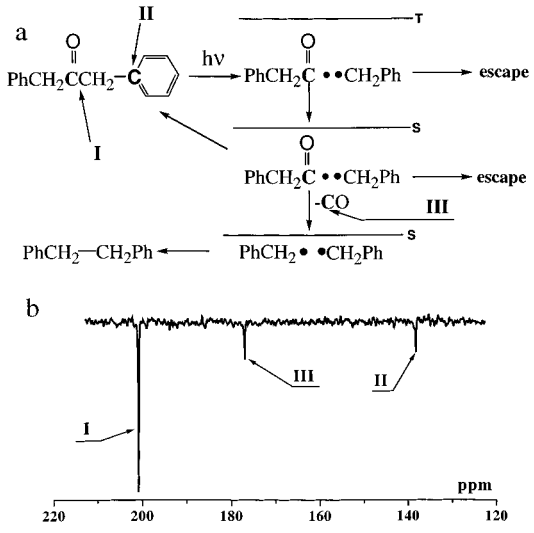

Figure 1. (a) Scheme of the DBK photolysis in the micelles. (b) CIDNP spectrum obtained upon photolysis of DBK in SDS micelles at salt addition (C_{NaCl}=0.1 M).

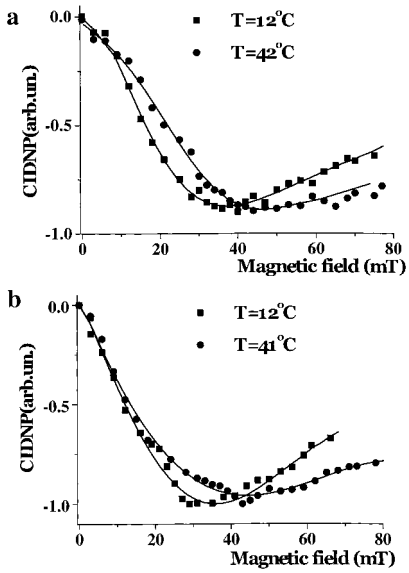

Figure 2. Magnetic field dependencies of CIDNP detected by the carbonyl ^{13}C NMR signal of MDB upon the photolysis of MDB in aqueous micellar solution of (a) SDS and (b) SOS at various temperatures. Solid curves are calculated CIDNP dependencies with the following parameters: $J_0 = 60$ mT, $\alpha = 2$ A^{-1}, and $k_s\tau = 1.6$. (a) $D = 5.1 \times 10^{-7}$ cm^2/s for $T = 12$ °C; $D = 2.3 \times 10^{-6}$ cm^2/s for $T = 42$ °C. (b)$D = 1.07 \times 10^{-6}$ cm^2/s for $T = 12$ °C; $D = 3 \times 10^{-6}$ cm^2/s for $T = 41$ °C.

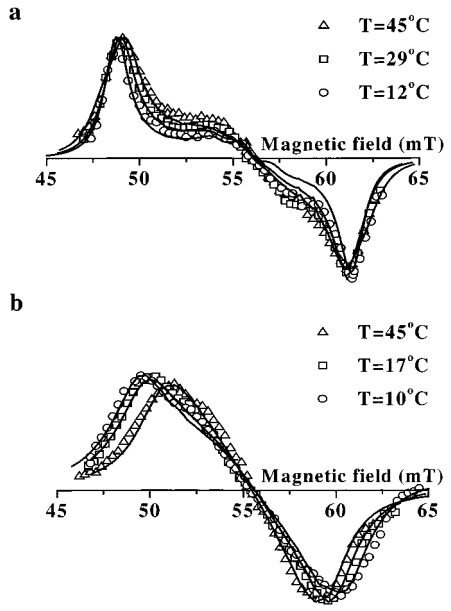

Figure 3. SNP spectra detected via carbonyl ^{13}C NMR signal of MDB upon the photolysis of MDB in (a) SDS and (b) SOS micelles at various temperatures. Solid lines are simulated spectra with following parameters: $J_0 = 60$ mT, $\alpha = 2$ A^{-1}, and $k_s\tau = 1.6$. The used values of L and D for SDS and SOS are listed in Tables 1 and 2, respectively.

TABLE 1: Temperature Dependence of the Experimental SNP Line Full Width at Half-Height ($\Delta\omega_{1/2}$) and Calculated Radius (L) of SDS Micelles and Diffusion Coefficient (D) of the Radical within the Micelle

T, °C	12	29	39	48
$\Delta\omega_{1/2}$, mT	1.8 ± 0.2	2.3 ± 0.1	2.6 ± 0.1	2.8 ± 0.1
L, Å	16.7	15.8	15.5	14.8
$D\cdot10^6$, cm^2/s	0.6	1.2	1.7	2.3

TABLE 2: Temperature Dependence of the Experimental Splitting in the SNP Spectrum ($\Delta\omega$) and Calculated Radius (L) of SOS Micelles and Diffusion Coefficient (D) of the Radical within the Micelle

T, °C	10	17	24	45
$\Delta\omega$, mT	10.8 ± 0.1	9.6 ± 0.2	8.2 ± 0.1	7.6 ± 0.1
L, Å	11.18	10.6	10.3	9.2
$D\cdot10^6$, cm^2/s	1.1	1.35	1.7	3.3

micelles are shown in Figure 3a,b. When MDB and DBK are photolyzed in SDS micelles, their ^{13}C SNP spectra exhibit the splitting of 12.3 ± 0.1 mT, which matches the respective hfi constant of the acyl carbon atom, and the variation of the temperature alters the line widths without affecting the observed splitting. At temperatures below 20° C, the SNP line width remains the same. The SNP spectra line widths for DBK and MDB in SDS micelles are equal at all temperatures within the experimental accuracy. The dependence of the SNP line full width at half-height is provided in Table 1.

At room temperature, the splitting in SNP spectrum detected for SOS micelles is equal to 8.3 ± 0.1 mT. As it has been shown in,[13,14] the decrease of splitting in SNP spectrum is caused by the growth of the reencounters rate. Reduced size of micelles leads to an increased ratio of times which RP spends in reactive and unreactive states and, hence, to increased time-averaged exchange interaction and time-averaged recombination rate. In smaller (SOS) micelles, the increase in temperature from 10 to 45° C decreases the splitting in the SNP spectrum from 10.8 to 7.6 mT (Table 2). Additionally, the SNP line width first increases and then starts to decrease as the temperature changes. Thus, qualitatively the temperature effect on SNP spectra shows the increase of the rate of reencounters as temperature grows.

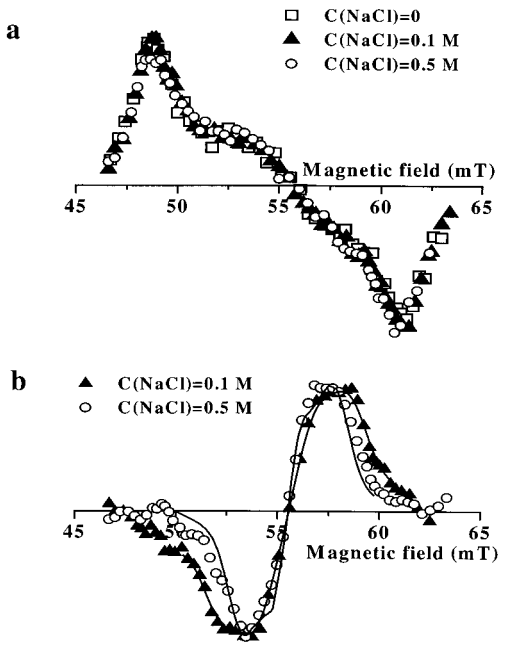

Figure 4. SNP spectra detected via (a) I and (b) II ^{13}C NMR signal of DBK upon the photolysis of DBK in SDS micelles at various concentrations of NaCl. Solid lines are simulated spectra with following parameters: $J_0 = 60$ mT, $\alpha = 2$ A^{-1}, and $k_s\tau = 1.6$.

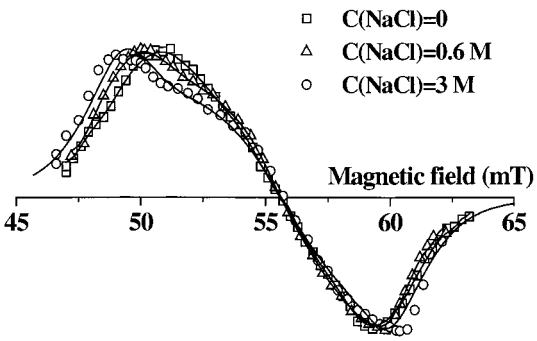

Figure 5. SNP spectra detected via carbonyl ^{13}C NMR signal of DBK upon the photolysis of DBK in SOS micelles at various concentrations of NaCl. Solid lines are simulated spectra with following parameters: $J_0 = 60$ mT, $\alpha = 2$ A^{-1}, and $k_s\tau = 1.6$. The used values of L and D for SOS are listed in Table 3.

Effect of NaCl on CIDNP and SNP Spectra. SNP spectra obtained upon DBK photolysis in SDS and SOS micelles with added NaCl are shown in Figures 4 and 5, respectively. NaCl additions have no effect on SNP spectra obtained via NMR line of carbonyl carbon ($A = 12.4$ mT) (Figure 4a). The main reason for that is the low sensitivity of SNP spectra to the changes in the rate of reencounters (Z) when $1/A \ll 1/Z$, which is the case for $A = 12.4$ mT in SDS micelles in the presence of NaCl. The NaCl addition leads to the decrease of the line width of SNP spectrum, detected via NMR line of ^{13}C (II) with $A = -1.4$ mT (Figure 4b), and to the substantial increase of SNP and CIDNP intensity, detected via NMR line of ^{13} CO (182 ppm).[42] The shape of the SNP spectrum detected by CO line is similar but of opposite phase to the SNP spectrum detected via carbonyl carbon of DBK. The difference in SNP spectra phases is explained by the difference in the pathway of product formation: incage for DBK and escape for CO. In SOS micelles, NaCl additions induced the increase of the splitting from 8.3 ± 0.1 mT at NaCl = 0 to 11.4 ± 0.1 mT at NaCl = 2.68 M (Table3) in full agreement with the expected behavior of the SNP spectrum upon the increase of micelle radius.

TABLE 3: Effect of NaCl on the Experimental Splitting in the SNP Spectrum ($\Delta\omega$) and Calculated Radius (L) of SOS Micelles and Diffusion Coefficient (D) of the Radical within the Micelle

C_{NaCl}, M	0	0.1	0.6	1.1	1.63	2.68
$\Delta\omega$, mT	8.29 ± 0.01	8.62 ± 0.03	9.64 ± 0.02	9.96 ± 0.03	10.11 ± 0.04	11.41 ± 0.02
L, Å	10.1	10.5	11.5	11.9	12.3	12.8
$D \cdot 10^6$, cm^2/s	1.7	1.7	1.5	1.4	1.25	1.15

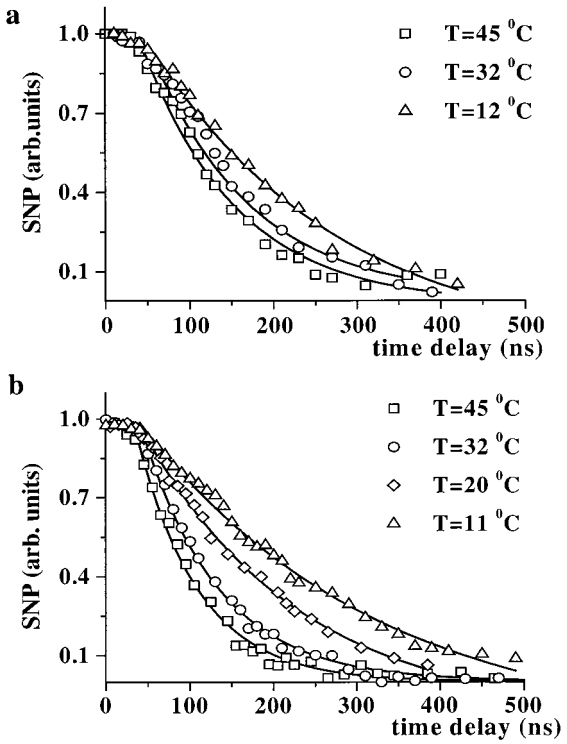

Figure 6. ^{13}C SNP kinetics upon the photolysis of MDB in (a) SDS and (b) SOS micelles at various temperatures. The observed rate constants k_{obs} for SDS and SOS are listed in Tables 4 and 5, respectively.

TABLE 4: Observed Decay Rate Constant (k_{obs}) Obtained in SDS Micelles

T, °C	12	29	32	45
$k_{obs} \cdot 10^{-6}$, s^{-1}	4.1 ± 0.3	7.4 ± 0.2	8.3 ± 0.3	12.0 ± 2.0

TABLE 5: Observed Decay Rate Constant (k_{obs}) obtained in SOS Micelles

T, °C	11	20	32	45
$k_{obs} \cdot 10^{-6}$, s^{-1}	4.2 ± 0.1	6.0 ± 0.2	9.9 ± 0.1	14.2 ± 1.5

Temperature Dependence of SNP Kinetics. Panels a and b of Figure 6 show the temperature dependence of the experimentally detected kinetics of micellized RP decay in MDB photolysis in SDS and SOS micelles, respectively. Except for the initial 60 ns of the curves, the SNP kinetics can be approximated reasonably well as single exponential decays. Avdievich et al.[43] have demonstrated that the initial nonexponential part of the kinetics is governed by the lifetime of the molecular triplets, which decay slowly ($k_T \approx 1.4-1.6 \times 10^7 c^{-1}$) to yield the RPs. The RP decay rate constants k_{obs} evaluated under the approximation of exponential RP decay in SDS and SOS micelles are summarized in Tables 4 and 5, respectively. The observed decay rate constant (k_{obs}) becomes larger at higher temperatures. The Arrhenius plot of the observed decay rates versus temperature is linear; the activation energies extracted from these plots are 6.8 ± 0.3 kcal/mol for SOS and 6.4 ± 0.3 kcal/mol for SDS micelles.

Effect of NaCl on SNP Kinetics. The salt additions have no effect on the decay rate of SNP kinetics of RPs formed in DBK photolysis in SDS. In SOS micelles the decay rate increased upon salt additions.

Calculation Model

For calculation of CIDNP and SNP spectra, model calculations based on the numerical solution of the Liouville equation[15] have been used. To describe the dynamics of RPs confined in the micelles, we employed the microreactor model.[44] It assumes that one of the radicals is permanently located at the center of a spherical micelle with radius L, whereas its partner diffuses freely within the micelle volume with diffusion coefficient D and escapes into water bulk. It is assumed that an escaped radical does not re-enter the same micelle. Along with the terms describing the Zeeman interaction of the electron spins and hfi, the Hamiltonian H_0 includes the term, describing the exchange interaction which exponentially depends on the interradical separation ($J(r) = J_0 e^{-(r-R_0)/\lambda}$). R_0 is the radius of the reaction zone. The characteristic length scale of the spatial overlap of electronic orbitals upon formation of chemical bonds was used as the parameter of the spatial decay of exchange interaction, $\lambda = 0.5$ Å. Two mechanisms of electron spin relaxation were taken into account: the dipole−dipole interaction of the electron spins and the fluctuations of the local magnetic fields (anisotropy of g- and hfi-tensors, spin−rotational coupling) characterized by the magnitude, G, and the rotational correlation time, τ_c. For acyl radicals, the main relaxation mechanism is the spin−rotational interaction,[45] which acts along with the relaxation induced by the anisotropic part of the hyperfine coupling. The anisotropic part of the Zeeman interaction can obviously be neglected, since the magnetic field B_0 is weak. The description of the relaxation caused by the fluctuation of the local magnetic fields follows the approach described earlier for the calculation of CIDNP magnetic field dependencies and SNP spectra of biradicals.[46] The two channels of the RP decay are considered: (i) an exponential decay, e.g., due to decarbonylation, and (ii) the escape of a radical from the micelle. The description of the dipole−dipole interaction was based on the approach developed by Steiner and Wu[47] and Morozov at al.[48] The differential scheme proposed by Pedersen and Freed[49] was employed to solve the equation. The RP recombination was characterized by dimensionless parameter $k_s\tau_s$, where $\tau_s = (R_{min}\delta)/D$ is an average RP residence time in the reaction zone of thickness δ. The values of J_0, $k_s\tau_s$, D, L, k_{esc}, G, and τ_c were treated as variables in the calculations performed.

Discussion

It has been shown earlier[14,15,13] that the most important factors which affect the shape of SNP spectra as well as CIDNP magnetic field dependencies are the electron exchange interaction, modulated by motion of radicals, and the rate of spin-selective RP decay. In large and relatively viscous micelles, the case of "slow motion" is realized. The rate of singlet−triplet conversion is higher than the rate of reencounters. In this case, the splitting in SNP spectra is equal to the hfi constant, A, while exchange interaction affects the line width of SNP spectra. The decrease of the micelle size leads to the increase of the rate of reencounters. In this "fast motion" case, the splitting in SNP

spectrum and line widths are determined by the ratio of the rate of reencounters, Z, and the hfi constant, A. In the limiting case, $A/Z \ll 1$, the splitting in SNP spectrum is equal to one-half of the hfi constant.

The reencounter frequency can be estimated as $Z = 4\pi R_0 D/V$; $V = 4\pi L^3/3-$ is the micelle volume.[37] For $A = 12.4$ mT and room temperature, this estimation gives $A/Z < 1$ for SDS (splitting in SNP spectrum is equal to the hfi constant) and $A/Z \gg 1$ for SOS (splitting in SNP spectrum is substantially less than the hfi constant).[13] For $A = 1.4$ mT, which corresponds to ^{13}C (II) nuclei, the same estimation gives $A/Z > 1$ for both SDS and SOS micelles at room temperature. Thus, the observed splitting in SNP spectrum, detected via the corresponding NMR line, is close to the half of hfi constant. Note that the sensitivity of SNP spectra detected via different NMR lines (which correspond to nuclei with different values of hfi constants) to the changes in micelle size and intramicelle viscosity is different. This can be clearly seen in the experimental results obtained.

The obtained results show that the temperature increase leads to the changes of SNP spectra shape and magnetic field dependencies similar to the changes caused by the decreasing of micelle size. Thus, one can conclude that the temperature increase leads to the increase of the reencounter rate, while the salt addition leads to the decrease of reencounter rate. A temperature change and salt additions alter the micelle viscosity and therefore change D and the micelle size L as well. To obtain quantitative information about the temperature and salt-induced variation of micelle size and viscosity, we have compared the experimentally detected SNP spectra and magnetic field dependencies of CIDNP with the results of model calculations based on the numerical solution of the Liouville equation.

The shape of the calculated SNP spectrum is governed by J_0, $k_s\tau_s$, D, and L, whereas other variables merely affect its absolute intensity. Upon temperature variation and salt addition, the values of J_0 and $k_s\tau_s$ remain unchanged. For these parameters, we used the values $k_s\tau_s = 1.6$ and $J_0 = -60$ mT, evaluated in a number of earlier studies based on a similar mathematical model and the experimental studies of MARY and isotope effects and the SNP spectra.[13−15,37,38]

The shape of calculated SNP spectra is not sensitive to the rate constant of RP decay. This is confirmed experimentally by the fact that the line widths of SNP spectra obtained in DBK and MDB photolysis are the same at the same temperature. The observed lifetimes of the corresponding RPs differ by a factor of 3 because the main channel of decay of the primary RP in case of DBK is the decarbonylation process, whereas for MDB, it is the electron spin relaxation and escape of radicals from the micelle.

The changes in the shape of SNP spectra upon temperature variations and salt additions could not be caused by changes in electron spin relaxation rate caused by modulation of the anisotropic hfi and dipole−dipole and spin−rotational interaction. It has been demonstrated earlier that at the room-temperature electron spin relaxation rate caused by modulation of the anisotropic hfi, dipole−dipole and spin−rotational relaxation has negligible effect on the SNP spectra.[13,14]

We therefore conclude that the main cause of the line width variation in SNP spectra upon temperature changes and salt additions is the variation of the reencounter frequency, which affects the rate of the exchange-induced relaxation. As reencounter frequency depends on both micelle radius and diffusivity ($Z \approx D/L^3$), the agreement between calculated and experimental data could be achieved at different sets of L and D values. We used literature data for the aggregation number at various temperatures and salt concentrations to calculate the micelle radius. Using these values, we have obtained the temperature and salt additions dependence of translational diffusivity of radicals inside the micelle.

Assuming the spherical shape of micelles, we can calculate the volume of micelle core as $V_m = 4\pi L^3/3 = N_a V$. Here V is the volume of polymethylene chain of one detergent molecule. To obtain V, we have used the Tanford formula[50]: $V = 27.4 + 26.9N_c$; here, V is measured in Å^3, and N_c is number of carbon atoms in detergent molecule. N_c equals to 12 for SDS and 8 for SOS micelles. The dependence of L on N_a is described as

$$L = \sqrt[3]{3N_a(27.4 + 26.9N_c)/4\pi} \qquad (1)$$

The temperature dependence of N_a, obtained by small-angle neutron scattering (SANS),[23] and formula 1 lead to the conclusion that the temperature increase from 12 to 50 °C caused the decrease of micelle radius from 16.7 to 14.48 Å The calculation of L has been done using eq 1, taking into account the radical size. This means that the value obtained from eq 1 should be decreased by radical radius (∼3Å). However, since the radicals may also experience the Stern layer, the effective radius should be increased by 1.3 Å.[37] On the basis of these results, the diffusivity D of the radicals in the SDS micelles at various temperatures was evaluated from the comparison of the calculated and experimental SNP spectra and is listed in Table 1.

Unfortunately, we could not find any literature data on the temperature influence on N_a for SOS micelles. Taking into account the similar structure of detergent molecules of SDS and SOS, we assumed the temperature dependence of aggregation number of SOS micelles to be proportional to that of SDS micelles. It was proposed that the temperature increase from 10 to 50 °C leads to the decrease of N_a from 33 to 20 and thus to a decrease of the radius from 11.1 to 9.2 Å, with corrections $\Delta L = 1.3$ Å for taking into account the radical size. The rest of the variables (G, J_0, and $k_s\tau_s$) were identical to those used in the simulations of the results for SDS micelles. The comparison of the experimental data with the results of simulations has yielded the values for the diffusivity at various temperatures; they are summarized in Table 2.

The earlier studies[51] have revealed the significant influence of all of the variables (J_0, $k_s\tau_s$, D, L, k_{esc}, G, and τ_c) on the magnetic field dependencies of CIDNP formed in micellized RPs. A reasonable agreement between calculated, and experimental CIDNP field dependencies can be achieved using a number of different sets of these parameters. It is therefore impossible to make unambiguous conclusions regarding the temperature dependence of the micelle parameters on the basis of the modeling of the CIDNP field dependencies alone. Note that a number of parameters such as the lifetime of micellized RP, the electron spin relaxation of radicals, the rate of spin-selective reactions, and the size and viscosity of the micelles significantly affect the CIDNP magnetic field dependencies. For instance, the photolysis of DBK and MDB produces two RPs with very close hfi constants but substantially different lifetimes of radical centers, and the extrema of the two magnetic field dependencies differ by 5.0 mT[13,51], with the shorter RP lifetime corresponding to an extremum being in a lower magnetic field. Qualitatively, such behavior is explained through the accumulation of the polarization produced by the T$_$-S mechanism upon the increase of the RP lifetime, which leads to an increased number of reencounters. The increase in the micelle size upon the temperature decrease leads to a decreased rate of reencounters on one hand and to the prolonged RP lifetime on the other.

In addition, the change in the intramicellar viscosity alters the rate of the electron spin relaxation. Thus, while the observed behavior demonstrates on the qualitative level that the micelle size becomes larger at lower temperatures, the evaluation of the quantitative parameters from the comparison of experimental and simulated results is not feasible. At the same time, the agreement of the experimental and calculated CIDNP field dependencies can serve as an additional confirmation of the results obtained from the modeling of SNP spectra.

The Arrhenius plot of D versus temperature is linear; the activation energy extracted from this plot is $E_a = 6.7 \pm 0.25$ kcal/M for SDS and $E_a = 5.6 \pm 0.2$ kcal/M for SOS. These values are very close to those obtained in [24] $E_a = 5.8$ kcal/M, where dibenzyl ester was used as a fluorescence probe. Note that the size of dibenzyl ester is close to the size of radicals used in this work. The activation energies obtained in our work are in good agreement with the activation energies for the rotational correlation times τ_c of the nitroxide radicals,[29] ($E_a =$ 6.5 kcal/mol for SDS and $E_a = 5.9$ kcal/mol for SOS). At the same time, the E_a obtained in this work is substantially different from the data obtained by Zana, $E_a = 10$ kcal/M,[26] where dipyrenylpropane has been used as a probe. The size of dipyrenylpropane is more than twice as large than the radicals investigated in this work. The substantial difference in activation energies obtained in our work and using the probe molecules of larger sizes is very probably determined by the influence of the probe molecules on the micelle interior the preferential localization of probe molecules in definite sites of micelle. The value of viscosity, evaluated using Debye−Stokes−Einstein formula $\eta = (3\tau_c kT)/(4\cdot\pi\cdot a^3)$ (here a is the hydrodynamic radius of the probe) and τ_c measured in ref 29 is in good agreement with our data if we take into account the differences in the radical radius. As it has been mentioned above, the shape of the SNP spectra is determined by the rate of reencounters, and thus, the translational motion of radicals determines the obtained viscosity only. The good agreement between our experimental data and the viscosity obtained using rotational correlation times of radicals of sizes close to those used in our work shows the applicability of the Debye−Stokes−Einstein formula for a micelle. Thus, despite the substantial heterogeneity of micelle interior, the translational and rotational correlation times for the radicals with radius of 1.5−3 Å are similar.

It is known[19,22,23] that SDS micelles grow as a function of the concentration of salt addition. The experimental dependence of aggregation number N_a on the total concentration of Na^+ (Y_{aq}) is well described by the formula[22] $N_a = 164(Y_{aq})^{1/4}$. Y_{aq} may be found from the conventional pseudophase ion exchange mass balance relationship $Y_{aq} = \alpha[SDS] + (1 - \alpha)[SDS]_{free} + [NaCl]$, where α is the apparent degree of counterion dissociation, $\alpha = 0.27$, and $[SDS]_{free}$ is the concentration of monomeric SDS. $[SDS]_{free}$ is calculated iteratively from eq 5 of ref 22. For micelle radius calculation, we used eq 1. For SOS, the aggregation number increases with increasing of salt concentration $N_a = K_2*(\alpha[SOS] + \beta[SOS]_{free} + [NaCl])^{\gamma}$, where[22] $K_2 =$ 38.5, $\gamma = 0.22$, $\beta = 0.655$, and $\alpha = 1 - \beta$. $[SOS]_{free}$'s are calculated iteratively from eq 5 of ref 22.

After calculation of N_a according to the abovementioned formula, the dependence of radius on salt concentration was obtained using eq 1. As it was mentioned above, the sensitivity of SNP spectrum on the rate of reencounters substantially depends on the value of hfi constant. The growth of micelle size upon salt addition leads to the decrease of the rate of reencounters but negligibly affects the line width of SNP spectrum detected via carbonyl carbon. The diffusivity (D) of radical in the SDS and SOS micelles at various concentrations of NaCl was obtained from the comparison of the calculated and experimental spectra (Figure 5). The radius of SDS micelles at NaCl concentrations 0.1 and 0.5 M were used as 18.3 and 20.8 Å. The corresponding diffusion coefficients D obtained were 0.8×10^{-6} and 0.6×10^{-6} cm^2/s. It is known that salt additions change the micelle shape from spherical to rodlike.[17,19,20] At salt concentration [NaCl] > 0.1 M and detergent concentration equal to 0.1 M, the shape of SDS micelles is not spherical but rodlike. The application of the theoretical model used is not fully correct, and obtained values of D for SDS micelles can be considered as estimations only. The results obtained for SOS micelles are more reliable because the shape of SOS micelles is very close to spherical at the concentrations of salt and detergent[20] used in this work.

Temperature Dependence of SNP Kinetics. The analysis of the SNP kinetics carried out by means of the numerical solution of the Liouville equation[39] has shown that for a rapid recombination of the RP from the singlet state, the value of k_{obs} is equal to the sum of the rate constants of relaxation (k_{rel}) and escape from the micelle (k_{esc}).

The electron spin relaxation rate has contributions from the electron spin relaxation of individual radicals and from dipole−dipole electron spin relaxation between radicals. In the earlier study,[39] the relative contribution of the dipole−dipole relaxation k_{dd} at 50 mT magnetic field was estimated as 10%. The electron spin relaxation rate of alkyl radical[40,45] does not exceed 5×10^6 s^{-1}, and its contribution into SNP kinetics is negligible. The relaxation for the acyl radicals has contributions from the modulation of the g-tensor, the modulation of the hfi anisotropy, and spin−rotational relaxation. In magnetic fields of 50 mT, the contribution of former relaxation mechanism is negligible. The rate constant of hfi-induced relaxation for RPs can be evaluated[47] as $k_{hfi} = (A{:}A)\tau_c/12(1 + \omega_0^2\tau_c^2)$, where ω_0 is the magnitude of the magnetic field in frequency units, $A{:}A = \sum_{i=x,y,z}(A_i - A_{iso})^2$ is the hfi anisotropy, and τ_c is the correlation time of the modulation of the hfi anisotropy. Using the value of 10.96 mT^2 for the hfi anisotropy of the benzoyl radical and values of τ_c at different temperatures obtained via simulation of SNP spectra, we have estimated k_{hfi}. The temperature increase from 12 to 45 °C leads to k_{hfi} changes from 8×10^5 to 1.6×10^6, which is less than 20% of k_{obs}.

The negligibile role of hfi-induced and dipole−dipole relaxation contribution into k_{obs} is confirmed by the fact that the observed rate constant at room temperature at 60.8 mT ($k_{obs} = 7.1 \pm 0.5 \times 10^6$ s^{-1}) is very close to that same at 15 mT ($k_{obs} = 7.5 \pm 1.5 \times 10^6$ s^{-1}).[53] The calculated hfi-induced and dipole−dipole relaxation rates[47,48] should increase significantly on going from 15 to 60 mT. This leads to the conclusion that the temperature dependence of k_{obs} is determined by electron spin relaxation, which does not depend on the magnetic field and the radical escape rate. It is known that the main relaxation mechanism of acyl radicals is the relaxation caused by the modulation of the spin−rotational interaction. As the correlation time of spin−rotational interaction is $\tau_{sr} \approx 10^{-11}-10^{-14}$ s, the parameter $\omega_0\tau_{sr} \ll 1$, and the rate constant of spin−rotational relaxation for RPs does not depend on magnetic field in range of 15−60 mT. TR EPR measurements of the electron relaxation time T_1 of benzoyl radical in different solvents show the slight increase of about 20% with increasing viscosity from pentane ($\eta = 0.2$ cP), $T_1 = 120$ ns, to dibuthylphtalate ($\eta = 17.7$ cP), $T_1 = 200$ ns.[53] The contribution of electron relaxation rate due to spin−rotational interaction into k_{obs} could be estimated as $k_{rel} = {}^1/_2T_1 \approx 2.2 \times 10^6$ s^{-1} and does not change much in our

temperature range. Thus, we believe that the temperature dependence of k_{obs} is mainly determined by changes in radical escape rate $k_{esc}(T)$. This conclusion is confirmed by the fact that the activation energy $E = 6.4 \pm 0.3$ kcal/mol of the observed decay rate is very close to the activation energy of the escape rate of ketyl radical in SDS micelles $E = 6.5 \pm 1.8$ kcal/mol obtained Evans et al.[54]

Effect of NaCl on SNP Kinetics. The addition of NaCl has no effect on SNP kinetics in SDS micelles and increases the decay rates of SNP kinetics in SOS. The RP lifetime in the case of DBK photolysis is mostly determined by decarbonylation rate. As is known,[55] the decarbonylation rate significantly depends on polarity: the increase of polarity leads to the decrease of decarbonylation rate. Thus, the main salt effect consists of the changes in the decarbonylation rate due to the decrease of polarity of the micelle interior. The micelle interior consists of the internal core with very low permeability for water molecules and the regions where the concentration of water is higher. The polarity of micelle interior regions close to the micelle surface at different concentrations of NaCl has been studied in the work of Bales et al.[19] It has been shown that the salt additions caused the micelle size growth due to the increase of the aggregation number. As a result, the distance between the charge heads of detergent molecules decreases. This in turn leads to the decreasing of water concentration in micelle interior. The observed decay rate for SDS micelles is equal to $K_{obs} = 1.1 \times 10^7\ s^{-1}$ and is in a good agreement with literature data for decarbonylation rate in nonpolar solvents.[55] The independence of the decay rate for SDS micelles on NaCl concentration (0.1−0.5 M) leads to the conclusion that the changes of polarity averaged over the volume of micelle interior are negligible. For smaller SOS micelles, the changes in the interior polarity are substantial, which leads to the increase of decay rate by about a factor of 1.7 when NaCl concentration changes from 0.025 to 1.1 M. Note that in the absence of decarbonylation reaction, the increase in the observed rate is expected due to the growth of micelle size upon salt additions.

Conclusions

Using the temperature dependence of the SNP spectra detected upon MDB and DBK photolysis in SDS and SOS micelles as a representative example, we have demonstrated that the SNP spectra of the micellized RPs are very sensitive to the temperature variations and therefore can be used as a probe for investigating translational diffusion of reacting radicals inside micelles. The temperature dependence of diffusivity for micellized radicals has been determined from the comparison of the experimental data with the calculations based on the numerical solution of the Liouville equation for the microreactor model. It has been shown that the temperature dependence of translational diffusion coefficient obtained via simulation SNP spectra of micellized radical pairs is the same as the temperature dependence of diffusion coefficient obtained using rotational correlation time of stable nitroxide radicals of similar sizes.

The time-resolved SNP technique has been employed to measure the temperature dependence of decay rate constants of the micellized RPs. We have shown that the temperature dependence of RP lifetimes is mainly determined by changes in radical escape rate.

Acknowledgment. The authors thank INTAS 99-1766 and the Russian Foundation for Basic Research Grants N 99-03-33488 and 99-03-32459 for financial aid.

References and Notes

(1) Gould, I. R.; Zimmt, M. B.; Turro, N. J.; Baretz, B. H.; Lehr, G. F. *J. Am. Chem. Soc.* **1985**, *107*, 4607.
(2) Turro, N. J.; Tarasov, V. F.; Buchachenko, A. L. *Accounts Chem. Res.* **1995**, *28*, 69.
(3) McLauchlan, K. A.; Nattrass, S. R. *Mol. Phys.* **1988**, *65*, 1483.
(4) Turro, N. J. *Pure Appl. Chem.* **1981**, *53*, 259.
(5) Closs, G. L.; Forbes, M. D. E.; Norris, J. R. *J. Phys. Chem.* **1987**, *91*, 3592.
(6) Weis, V.; van Willigen, H. J. *Porphyrins Phthalocyanines*, **1998**, *2*, 353.
(7) Van Willigen, H.; Levstein, P. R.; Martino, D.; Ouardaoui, A.; Tassa, C. *Appl. Mag. Reson.* **1997**, *12*, 395.
(8) Wu, J. Q.; Baumann, D.; Steiner, U. E. *Mol. Phys.* **1995**, *85*, 981.
(9) Zimmt, M. B.; Doubleday, C., Jr.; Turro, N. J. *J. Am. Chem. Soc.* **1984**, *106*, 3363.
(10) Batchelor, S. N.; McLauchlan, K. A.; Shkrob, I. A. *Z. Phys. Chem.* **1993**, *180*, 9.
(11) Okazaki, M.; Sakata, S.; Konaka, R.; Shiga, T. *J. Chem. Phys.* **1987**, *86*, 6792.
(12) Polyakov, N. E.; Okazaki, M.; Toriyama, K.; Leshina, T. V.; Fujiwara, Y.; Tanimoto, Y. *J. Phys. Chem.* **1994**, *98*, 10563.
(13) Bagryanskaya, E. G.; Sagdeev, R. Z. *Z. Phys. Chem.* **1993**, *180*, 111.
(14) Tarasov, V. F.; Bagryanskaya, E. G.; Shkrob, I. A.; Avdievich, N. I.; Ghatlia, N. D.; Lukzen, N. N.; Turro, N. J.; Sagdeev, R. Z. *J. Am. Chem. Soc.* **1995**, *117*, 110.
(15) Bagryanskaya, E. G.; Tarasov, V. F.; Avdievich, N. I.; Shkrob, I. A. *Chem. Phys.* **1992**, *162*, 213.
(16) Bagryanskaya, E. G.; Sagdeev, R. Z. *Prog. React. Kinet.* **1993**, *18*, 63.
(17) Mazer, N. A.; Benedek, G. B.; Carey, M. C. *J. Phys. Chem.* **1976**, *80*, 1075.
(18) Malliaris, A.; Le Moigne, J.; Sturm, J.; Zana, R. *J. Phys. Chem.* **1985**, *89*, 2709.
(19) Bales, B. L.; Messina, L.; Vidal, A.; Peric, M.; Nascimento, O. R. *J. Phys. Chem. B* **1998**, *102*, 10347.
(20) Missel, P. J.; Mazer, N. A.; Benedek, G. B.; Carey, M. C. *J. Phys. Chem.* **1983**, *87*, 1264.
(21) Croonen, Y.; Gelade, E.; Van der Zegel, M.; Van der Auweraer, M.; Vandendriessche, H.; De Schryver, F. C.; Almgren, M. *J. Phys. Chem.* **1983**, *87*, 1426.
(22) Quina, F. H.; Nassar, P. M.; Bonilha, J. B. S.; Bales, B. L. *J. Phys. Chem.* **1995**, *99*, 17028.
(23) Bezzobotnov, V. Y.; Borbely, S.; Cser, L.; Farago, B.; Gladkih, I. A.; Ostanevich, Y. M. *J. Phys. Chem.* **1988**, *92*, 5738.
(24) Emert, J.; Behrens, C.; Goldenberg, M. *J. Am. Chem. Soc.* **1979**, *101*, 771.
(25) Zachariasse, K. A. *Chem. Phys. Lett.* **1978**, *57*, 429.
(26) Zana, R. *J. Phys. Chem. B* **1999**, *103*, 9117.
(27) Turro, N. J.; Okubo, T. *J. Am. Chem. Soc.* **1981**, *103*, 7224.
(28) Ottaviani, M. F.; Baglioni, P.; Martini, G. *J. Phys. Chem.* **1983**, *87*, 3146.
(29) Wasserman, A.; Tarasov V. F.; et al. *Chem. Phys.*, in press.
(30) Tarasov, V. F.; Forbes, M. D. E. *Spectrosc. Acta* **2000**, *56*, 245.
(31) Ellena, J. F.; Dominey, R. N.; Cafisto, D. S. *J. Phys. Chem.* **1987**, *91*, 131.
(32) Lehr, G. R.; Turro, N. J. *Tetrahedron* **1981**, *37*, 3411.
(33) Angel, P. S. *J. Am. Chem. Soc.* **1970**, *92*, 6074.
(34) Mckenzie, A.; Roger, R.; Wills, G. O. *J. Chem. Soc.* **1927**, 779.
(35) Lunazzi, L.; Ingold, K. U.; Scaiano, J. C. *J. Phys. Chem.* **1983**, *87*, 529.
(36) Turro, N. J.; Gould, I. R.; Baretz, B. H. *J. Phys. Chem.* **1983**, *87*, 531.
(37) Tarasov, V. F.; Ghatlia, N. D.; Buchachenko, A. L.; Turro, N. J. *J. Am. Chem. Soc.* **1992**, *114*, 9517.
(38) Tarasov, V. F.; Ghatlia, N. D.; Avdievich, N. I.; Shkrob, I. A.; Buchachenko A. L.; Turro, N. J. *J. Am. Chem. Soc.* **1994**, *116*, 2281.
(39) Parnachev, A. P.; Bagryanskaya, E. G.; Tarasov, V. F.; Lukzen, N. N.; Sagdeev, R. Z. *Chem. Phys. Lett.* **1995**, *244*, 245.
(40) Paul, H.; Fischer, H. *Helv. Chim. Acta* **1973**, *56*, 1575.
(41) Turro, N. J.; Anderson, D. R.; Chow, M.-F.; Chung, C.-J.; Kraeuntler, B. *J. Am. Chem. Soc.* **1981**, *103*, 3892.
(42) Ettinger, R.; Blume, P.; Patterson, A.; Lauterbur, P. C. *J. Chem. Phys.* **1960**, *33*, 1597.
(43) Avdievich, N. I.; Bagryanaksya, E. G.; Tarasov, V. F.; Sagdeev, R. Z. *Z. Phys. Chem. Board* **1993**, *182*, 107.
(44) Tarasov, V. F.; Buchachenko, A. L.; Maltzev, V. I. *Russ. J. Phys. Chem.* **1981**, *55*, 1921.
(45) Paul, H. *Chem. Phys. Lett.* **1975**, *160*, 472.
(46) Koptyug, I. V.; Lukzen, N. N.; Bagryanskaya, E. G.; Doktorov, A. B.; Sagdeev, R. Z. *Chem. Phys.* **1992**, *162*, 165.

(47) Steiner, U. E.; Wu, J. R. *Chem. Phys.* **1992**, *162*, 53.
(48) Morozov, V. A.; Isakov, S. V.; Sagdeev, R. Z. *Chem. Phys. Reports* **1997**, *16*, 559.
(49) Pedersen, J. B.; Freed, J. H. *J. Chem. Phys.* **1974**, *58*, 2746.
(50) Tanford, C. *J. Phys. Chem.* **1972**, *76*, 3020.
(51) Shkrob, I. A.; Tarasov, V. F.; Bagryanskaya, E. G. *Chem. Phys.* **1991**, *153*, 427.
(52) Fedin, M. V.; Bagryanskaya, E. G.; Purtov, P. A. *J. Chem. Phys.* **1999**, *111*, 5493.
(53) Bagryanskaya, E. G.; Makarov, T. V.; Paul, H. Unpublished results.
(54) Evans, C. H.; Scaiano, J. C.; Ingold, K. U. *J. Am. Chem. Soc.* **1992**, *114*, 140.
(55) Tsentalovich, Y. P.; Fisher, U. *J. Chem. Soc., Perkin Trans. 2* **1994**, 729.